



THE UNIVERSITY *of* EDINBURGH

Edinburgh Research Explorer

## Identification of alternative splicing events related to fatty liver formation in duck using full-length transcripts

### Citation for published version:

Wang, Y, Song, L, Ning, M, Hu, J, Cai, H, Song, W, Gong, D, Liu, L, Smith, J, Li, H & Huang, Y 2023, 'Identification of alternative splicing events related to fatty liver formation in duck using full-length transcripts', *BMC Genomics*, vol. 24, no. 92, pp. 1-13. <https://doi.org/10.1186/s12864-023-09160-4>

### Digital Object Identifier (DOI):

[10.1186/s12864-023-09160-4](https://doi.org/10.1186/s12864-023-09160-4)

### Link:

[Link to publication record in Edinburgh Research Explorer](#)

### Document Version:

Peer reviewed version

### Published In:

BMC Genomics

### General rights

Copyright for the publications made accessible via the Edinburgh Research Explorer is retained by the author(s) and / or other copyright owners and it is a condition of accessing these publications that users recognise and abide by the legal requirements associated with these rights.

### Take down policy

The University of Edinburgh has made every reasonable effort to ensure that Edinburgh Research Explorer content complies with UK legislation. If you believe that the public display of this file breaches copyright please contact [openaccess@ed.ac.uk](mailto:openaccess@ed.ac.uk) providing details, and we will remove access to the work immediately and investigate your claim.



1 **Title: Identification of alternative splicing events related to fatty liver**  
2 **formation in duck using full-length transcripts**

3 Yiming Wang<sup>1†</sup>, Linfei Song<sup>1†</sup>, Mengfei Ning<sup>1</sup>, Jiaxiang Hu<sup>1</sup>, Han Cai<sup>1</sup>, Weitao Song<sup>2</sup>,  
4 Daoqing Gong<sup>3</sup>, Long Liu<sup>3</sup>, Jacqueline Smith<sup>4</sup>, Huifang Li<sup>2\*</sup> & Yinhua Huang<sup>1\*</sup>

5 <sup>1</sup>State Key Laboratory for Agrobiotechnology, College of Biology Sciences, China  
6 Agricultural University, Beijing, China.

7 <sup>2</sup>Department of Waterfowl Breeding and Production, Jiangsu Institute of Poultry  
8 Science, Yangzhou, China.

9 <sup>3</sup>College of Animal Science and Technology, Yangzhou University, Yangzhou, China.

10 <sup>4</sup>The Roslin Institute and Royal (Dick) School of Veterinary Studies, University of  
11 Edinburgh, Midlothian, EH25 9RG, UK

12 \*To whom correspondence shall be addressed:

13 Prof. Yinhua Huang

14 State Key Laboratory for Agrobiotechnology, College of Biology Sciences, China  
15 Agricultural University

16 No.2 Yuan Ming Yuan West Road, Hai Dian District, Beijing 100193, China

17 Tel: 0086 10 6273 3123; Fax: 0086 10 6273 3904

18 Email: cauhyh@cau.edu.cn

19 Dr. Huifang Li

20 Department of Waterfowl Breeding and Production, Jiangsu Institute of Poultry  
21 Science

22 No. 58 Cangjie Road, Hanjiang District, Yangzhou, 349019093, China.

23 Tel: 0086 514 8559 9228

24 Email: lhxf\_002@aliyun.com

25 †Authors contributed equally to this work.

26 **Abstract**

27 **Background:** Non-alcoholic fatty liver disease (NAFLD) is one of most common  
28 diseases in the world. Recently, alternative splicing (AS) has been reported to play a  
29 key role in NAFLD processes in mammals. Ducks can quickly form fatty liver similar  
30 to human NAFLD after overfeeding and restore to normal liver in a short time,  
31 suggesting that ducks are an excellent model to unravel molecular mechanisms of  
32 lipid metabolism for NAFLD. However, how alternative splicing events (ASEs) affect  
33 the fatty liver process in ducks is still unclear.

34 **Results:** Here we identify 126,277 unique transcripts in liver tissue from an overfed  
35 duck (77,237 total transcripts) and its sibling control (69,618 total transcripts). We  
36 combined these full-length transcripts with Illumina RNA-seq data from five pairs of  
37 overfed ducks and control individuals. Full-length transcript sequencing provided us  
38 with structural information of transcripts and Illumina RNA-seq data reveals the  
39 expressional profile of each transcript. We found, among these unique transcripts,  
40 30,618 were lncRNAs and 1,744 transcripts including 155 lncRNAs and 1,589 coding  
41 transcripts showed significantly differential expression in liver tissues between  
42 overfed ducks and control individuals. We also detected 27,317 ASEs and 142 of them  
43 showed significant relative abundance changes in ducks under different feeding  
44 conditions. Full-length transcript profiles together with Illumina RNA-seq data  
45 demonstrated that 10 genes involving in lipid metabolism had ASEs with significantly  
46 differential abundance in normally fed (control) and overfed ducks. Among these  
47 genes, protein products of five genes (*CYP4F22*, *BTN*, *GSTA2*, *ADH5*, and *DHRS2*

48 genes) were changed by ASEs.

49 **Conclusions:** This study presents an example of how to identify ASEs related to  
50 important biological processes, such as fatty liver formation, using full-length  
51 transcripts alongside Illumina RNA-seq data. Based on these data, we screened out  
52 ASEs of lipid-metabolism related genes which might respond to overfeeding. Our  
53 future ability to explore the function of genes showing AS differences between  
54 overfed ducks and their sibling controls, using genetic manipulations and  
55 co-evolutionary studies, will certainly extend our knowledge of genes related to the  
56 non-pathogenic fatty liver process.

57 **Keywords:** full-length transcripts sequencing, duck, fatty liver, alternative splicing

## 58 **Background**

59 In humans, non-alcoholic fatty liver disease (NAFLD) is one of the most common  
60 global diseases with the overall incidence being 46.9 cases per 1000 people per year  
61 in a recent survey [1]. NAFLD has clinical-pathological symptoms including isolated  
62 steatosis, non-alcoholic steatohepatitis (NASH) and liver fibrosis [2]. The possibility  
63 of NAFLD is higher in men and increases with advancing age. NAFLD in obese  
64 children and adolescents further develops into more serious diseases [3, 4]. Similarly,  
65 intake of energy-rich food induces fatty liver in ducks, which shows the same  
66 pathology with human NAFLD [5, 6]. However, ducks can recover from fatty liver  
67 quickly and protect their liver against pathological changes such as fibrosis and  
68 ultimately cirrhosis that frequently happen in human NAFLD [7-9]. Therefore, ducks  
69 provide a good model to unravel the molecular mechanisms underlying lipid  
70 metabolism and hepatic steatosis.

71 Alternative splicing is one of the most important events that regulate function of  
72 proteins through generating different transcript isoforms. Alternative splicing has been  
73 reported in many bioprocesses including human ageing, human cancer and sex  
74 selection of birds [10-12]. Alternative splicing also plays an important role in NAFLD  
75 and dysregulation of alternative splicing contributes to development of NAFLD  
76 [13-15]. For example, DRAK2 inhibits SRPK1-mediated SRSF6 phosphorylation and  
77 leads to changes of SRSF6-associated alternative splicing of mitochondrial  
78 function-related genes to aggravate NALFD procedure [16]. To our knowledge,  
79 studies on fatty liver of ducks have been focused on genes related to lipid metabolism

80 based on RNA-seq short read data or explored nutrition complement affecting fat  
81 deposition in duck liver. [17-20]. However, the role of alternative splicing is unclear  
82 in process of responding to fatty liver of duck. Here we performed full-length  
83 transcript sequence using a pair of sibling ducks, which were fed with high fat corn  
84 feed and commercial forage, respectively. We annotated transcripts and compared  
85 their expression in liver tissues of overfed and control ducks. This effort identified  
86 27,317 ASEs, with 142 of them having significant frequency changes in liver tissues  
87 between overfed and control ducks. Moreover, we have identified five lipid  
88 metabolism related genes (*CYP4F22*, *BTN*, *GSTA2*, *ADH5*, and *DHRS2* genes) from  
89 these 142 events. These observations revealed the probable ASEs regulating the  
90 formation and defense process of liver in avoiding pathogenic fatty liver disease.

## 91 **Results**

### 92 **PacBio full-length high-coverage liver transcriptomic profile of overfed and** 93 **control ducks**

94 We sequenced liver transcriptomes of a sib-pair ducks using the PacBio Sequel  
95 platform. This identified 172,671 and 185,070 full-length transcripts from 6,327,390  
96 subreads of overfed duck and 6,716,303 subreads of control individuals, respectively.  
97 We then identified 77,237 and 69,618 unique transcripts from liver tissues of overfed  
98 and control ducks respectively, and merged these transcripts into a single data set  
99 containing 126,277 unique transcripts (Fig. 1a). Alignment of 77,237 and 69,618 liver  
100 transcripts of overfed and control ducks to our duck reference gene set showed that  
101 9,554 and 9,515 genes were expressed, respectively. These numbers of expressed

102 genes covered 82.05% and 82.88% genes detected by Illumina RNA-seq data in  
103 overfed and control ducks (unpublished data), suggesting that these two full-length  
104 transcriptomes were high coverage and provided a reasonable substrate for the  
105 analysis presented in this study. Sequence alignment of 126,277 unique transcripts to  
106 our new duck assembly (SKLA1.0, PRJNA792297) and gene reference set showed  
107 that 27.01% of them were unique transcripts, while 72.99% have different transcripts  
108 (Fig. 1b). The average number of exons was 6.4, the average length of these 126,277  
109 unique transcripts 3,864 bp and 27,410 transcripts had more than 10 exons (Fig. 1c).  
110 When compared to our duck reference gene sets, a total of 81,246 transcripts were  
111 mapped to 10,888 genes and 45,031 transcripts were novel transcripts (Fig. 1d).  
112 Among these 45,031 novel transcripts, 30,512 were annotated as novel transcripts of  
113 lncRNAs and 14,519 were annotated as novel transcripts of coding genes. Moreover,  
114 302 transcripts were intra-chromosomal fusion transcripts. These data suggested that  
115 our full-length transcriptome was a rich source of biological diversity.

#### 116 **Comparison of transcript expression between overfed and control ducks**

117 We compared full-length liver transcriptomic profiles of the above sib-pair ducks.  
118 This effort found 56,659 transcripts uniquely presented in overfed ducks, 49,040  
119 transcripts only presented in control ducks and 20,578 transcripts were observed in  
120 both overfed and control ducks (Fig. 2a). We further counted expression levels of  
121 transcript by TPM (Transcripts per kilobase of exon model divided by million mapped  
122 reads) and identified 1,744 transcripts of 1,282 genes showing significantly  
123 differential expression (DETs, p-value < 0.01) in liver tissues between overfed and



124 control ducks (Additional file 1: Table S1). Among 1,744 DETs, 982 were upregulated  
125 and 762 were downregulated with  $p\text{-value} < 0.01$  in overfed ducks when compared to  
126 those in control ducks (Fig. 2b). Using thresholds of  $|\log_2\text{FC}| > 1$  (FC, Fold Change),  
127 we identified 683 being upregulated and 382 being downregulated in overfed ducks  
128 when compared to their sibling controls. Gene ontology (GO) analysis indicated that  
129 1,282 genes presenting DETs were enriched in 45 biological functions, with 27  
130 involved in fatty acid metabolic process (GO:0006631) with  $\text{FDR} < 0.05$  (Fig. 2c).  
131 KEGG analysis demonstrated that 9 genes showing DETs were enriched in  
132 biosynthesis of unsaturated fatty acids, fatty acid metabolism and fatty acid elongation  
133 pathway ( $p\text{-value} < 0.01$ , Fig. 2d). *FADS1* (Fatty Acid Desaturase 1) and *FADS2*  
134 (Fatty Acid Desaturase 2) were previously reported to reduce lipid accumulation and  
135 influence the NAFLD process in mice [21-25]. Interestingly, we found that transcript  
136 isoforms of *FADS1* (Fatty Acid Desaturase 1) TCONS\_00055559 and *FADS2* (Fatty  
137 Acid Desaturase 2) TCONS\_00057710 were significantly upregulated in overfed  
138 ducks when compared to those in control ducks. These results reveal detailed  
139 information of expression profiles of *FADS1* and *FADS2* at the transcript-level and  
140 identify the main transcripts of *FADS1* and *FADS2* which might function in the  
141 formation of fatty liver in ducks to alleviate liver injury. Moreover, we compared  
142 reference transcripts to the above 1,744 differentially expressed transcripts to verify  
143 the confidence of detected transcripts. We found 893 of these DETs, including  
144 TCONS\_00057710, were known transcripts of *FADS1*, while TCONS\_00055559 was  
145 a novel transcript of *FADS1*. Aligning all four reference FADS1 protein sequences to

146 TCONS\_00055559 protein sequence, we found that TCONS\_00055559 was a new  
147 recombination of FADS1 exons. This observation suggested that TCONS\_00055559  
148 was a new transcript of FADS1 in ducks (Additional file 2: Fig S1 and Additional file  
149 3: Table S2).

### 150 **Prediction of lncRNA and lncRNA-coding cis-acting pairs**

151 For the above 126,277 unique transcripts, 42,642 transcripts were predicted as  
152 non-coding sequences and 30,618 were annotated as lncRNA, including 155 DETs  
153 (Fig. 3a). We compared characteristics of lncRNA and protein-coding transcript  
154 isoforms. We found that lncRNA had lower mean expression level (TPM) than  
155 protein-coding transcripts did, in both control and overfed ducks (Fig. 3b). Among  
156 30,618 lncRNA transcripts, 12,861 did not overlap with coding genes and 17,757 did  
157 overlap with coding-genes. Detailed transcript structure analysis indicated, among  
158 these lncRNA transcripts, a few (2.13%) had more than three exons, a small  
159 percentage (11.64%) had two or three exons, and many (86.23%) had only one exon.  
160 This was different from the case of protein-coding transcripts, where most (59.70%)  
161 had more than three exons, a few (12.68%) had two or three exons and the remainder  
162 (27.62%) had only one exon (Fig. 3c). Moreover, we calculated the correlation  
163 between 155 lncRNA DET and adjacent protein-coding transcripts with 10 liver tissue  
164 RNA-seq transcriptomes. This analysis identified 57 lncRNA-coding cis-acting pairs,  
165 including 34 lncRNA and 52 protein-coding transcripts from 32 genes with a Pearson  
166 correlation higher than 0.8. Amongst these pairs, four genes (*ENPPI* (ectonucleotide  
167 pyrophosphatase 1), *SERPINA1* (serpin family A member 1), *MGAT2*

168 (alpha-1,6-mannosyl-glycoprotein 2-beta-N-acetylglucosaminyltransferase) and  
169 *SSU72* (RNA polymerase II CTD phosphatase) were reported to have close  
170 association with NAFLD process (Fig. 3d). Overexpression of *ENPP1* in mice leads  
171 to insulin resistance and *MGAT2* deficiency reduces lipid absorption and insulin  
172 resistance [26, 27]. *SERPINA1* was associated with severity of NAFLD and *SSU72*  
173 influenced NAFLD deterioration [28, 29]. It will therefore be of interest to study  
174 whether and how lncRNA interacts with these four genes to regulate the fatty liver  
175 process of ducks.

#### 176 **Identification of ASEs using duck full-length transcripts**

177 Alternative splicing always requires the spliceosome, which catalyzes splicing  
178 reactions [30]. Under the function of the spliceosome, transcripts undergo one or more  
179 forms of alternative splicing. We counted ASEs which included skipped exon (SE),  
180 mutually exclusive exons (MX), alternative 5'splice site (A5), alternative 3'splice site  
181 (A3) and retained intron (RI) (Additional file 2: Fig S2a). Among the above 126,277  
182 unique transcripts, we detected 27,317 ASEs in 5,665 genes, which included 18% RI,  
183 41% SE, 19% A3, 20% A5 and 2% MX (Additional file 2: Fig S2b). We aligned  
184 transcripts to our duck reference genome to define ASEs as known and novel classes.  
185 This found 26,979 ASEs in known reference genes and 338 ASEs in novel genes.

186 We then compared ASE characteristics in liver transcriptomes of overfed and  
187 control ducks. This analysis detected 20,823 ASEs in liver of control and 26,228 in  
188 overfed ducks. Amongst these, the liver of control duck had a large proportion of RI  
189 events (43%), a small proportion of SE (20%), A3 (18%) and A5 (17%), and a few

190 MX (2%). This is similar to the case in overfed ducks, where there was 41% RI, 20%  
191 SE, 18% A3, 19% A5 and 2% MX events (Fig. 4a). We then compared the number of  
192 transcript isoforms in liver transcriptomes and found that 9 genes (*ACATI*  
193 (acetyl-CoA acetyltransferase 1), *ACSL1* (acyl-CoA synthetase long chain family  
194 member 1), *CPT1A* (carnitine palmitoyltransferase 1A), *FADS2* (fatty acid desaturase  
195 2), *ACSL5* (acyl-CoA synthetase long chain family member 5), *PTPLADI*  
196 (3-hydroxyacyl-CoA dehydratase 3), *FASN* (fatty acid synthase), *ACOX1* (acyl-CoA  
197 oxidase 1) and *ACACA* (acetyl-CoA carboxylase alpha)) had different numbers of  
198 protein sequences between overfed and control ducks (Fig. 4b). Among them, *FASN*  
199 was a key enzyme in fatty acid biosynthesis, bound to FMN (Flavine Mononucleotide)  
200 cofactor via its DUS (Dihydrouridine synthase) domain to produce reactive oxygen  
201 species (ROS) in NADPH-dependent oxidation [31]. Interestingly, we found that  
202 *FASN* had a transcript ('overfed4' in Fig. 4c and Additional File 3: Table S3) which  
203 contained the DUS domain and expressed in livers of five overfed ducks, but was not  
204 detected in these of five control ducks (Fig. 4c). These observations together with  
205 overfed ducks with fatty liver did not present inflammation and fibrosis (unpublished  
206 data) suggesting that ducks might relieve the oxidative damage of fatty liver through  
207 AS of these genes.

### 208 **Significantly changed ASEs involved in lipid metabolism**

209 Transcript isoforms can have similar or antagonistic functions. For example, *MAVS*  
210 (mitochondrial antiviral signaling protein), a regulator of antiviral innate immunity,  
211 expresses two transcript isoforms, where the miniMAVS antagonizes the full-length

212 MAVS to induce interferon production [32]. Here we calculated the frequency  
213 changes of ASEs with expression profiles of transcript isoforms. We observed that  
214 five (*CYP4F22*, *BTN*, *GSTA2*, *ADH5*, and *DHRS2*) genes showed significant  
215 differential ASEs in liver transcriptomes of overfed ducks compared with control  
216 ducks (Additional file 2: Fig S3).

217 *CYP4F22* (cytochrome P450 family 4 subfamily F member 22) as a fatty acid  
218  $\omega$ -hydroxylase involved in lipid metabolism to maintain the skin barrier in mice [33].  
219 Signal peptides carry information for protein secretion and play an important role in  
220 human diseases [34-36]. Interestingly, we found overfed ducks preferred to express a  
221 transcript isoform with a signal peptide in its N-terminal, while control ducks  
222 preferred to express a transcript isoform without N-terminal signal peptide (Fig. 5a  
223 and Additional file 2: Fig S4a). We then evaluated the impact on biological function  
224 of an amino acid indel in transcript isoforms using PROVEAN software (score < 2.5  
225 indicates a harmful detrimental change) [37]. This suggested that deletion of 146  
226 amino acids at the N-terminal in *CYP4F22* transcript isoform TCONS\_00116966  
227 (with a score of -289.14), was suggested to be deleterious to *CYP4F22* function in  
228 ducks. We performed the cross-species alignment of *CYP4F22* proteins in six birds  
229 and found the N-terminal 24 amino acids showed low conservation, while the  
230 remainder of the sequences were relatively conserved in the N-terminal 200 amino  
231 acids of *CYP4F22* proteins (Fig. 5b and Additional file 3: Table S4). Since the  
232 transcript isoform of *CYP4F22* which missing the signal peptide are preferred in  
233 control ducks, we inferred that ASEs might regulate secretion or localization of

234 CYP4F22 proteins by alternative splicing. We also noticed an A5 ASEs in a *BTN* gene,  
235 which had been reported to regulate milk-lipid secretion in mice [38]. The alternative  
236 transcript TCONS\_00099256 encoded a 513aa (amino acid) longer protein and was  
237 expressed at lower levels, while TCONS\_00099264 had a 209aa truncation of the  
238 cytoplasmic domain and was expressed more highly in overfed ducks when compared  
239 to that in control individuals (Fig. 5c and Additional file 2: Fig S4b). Furthermore, we  
240 found that the B30.2 domain was lost in the TCONS\_00099264 encoding protein  
241 (Additional file 2: Fig S4c). *ADH5* (alcohol dehydrogenase 5 class-3, also called  
242 ADH-3) has been shown to protect the liver from the damage of nonalcoholic hepatic  
243 steatosis in mice [39]. We found an ASE event in the *ADH5* gene of ducks leading to  
244 a 122aa truncation in the N-terminal of the protein and having deleterious  
245 consequences on protein function (-459.358 Provean score) (Fig. 5d and Additional  
246 file 2: Fig S4d). Cross-species sequence alignment analysis showed ADH5 proteins  
247 were highly conserved (Fig. 5e). The frequency of this ASE event was lower in  
248 overfed ducks, thus overfed ducks had more full-length transcripts of ADH5 protein.  
249 The *GSTA2* gene functions in detoxification of electrophilic compounds such as H<sub>2</sub>O<sub>2</sub>  
250 or other products of oxidative stress [40]. The relative abundance of an A3 event in  
251 *GSTA2* was observed to be lower in control individuals (Additional file 2: Fig S3).  
252 However, no obvious change was identified during Phobius analysis of the alternative  
253 transcripts (TCONS\_00036568) of the *GSTA2* gene (Additional file 2: Fig S4e and  
254 Additional file 2: Fig S5a). The results from Provean show limited expected harm of  
255 the short protein sequence change, suggesting a relatively slight effect of the protein

256 truncation (-13.715 score). Therefore, this A3 event has less influence on *GSTA2*  
257 protein function. The *DHRS2* gene localizes in the mitochondria and plays a role in  
258 oxidation–reduction processes [41]. An N-terminal truncation by an ASE event was  
259 found in the *DHRS2* gene in ducks, with the frequency of this ASE event being lower  
260 in overfed ducks. Thus overfed ducks express more full-length transcript of the  
261 *DHRS2* gene (Additional file 2: Fig S3). We showed the selective N-terminal  
262 truncation of predicted DHRS2 protein sequences (Additional file 2: Fig S4f). The  
263 alignment of DHRS2 protein in duck with another five species shows that the 1-100aa  
264 region has relatively higher conservation (Additional file 2: Fig S5c). Provean  
265 predicts the potentially harmful result of this truncation with a score of -312.288.  
266 Under the overfed condition, ducks reduced levels of the truncated protein and  
267 increased expression of the full-length protein of the *DHRS2* gene.

## 268 **Discussion**

269 Ducks provide a good model for the study of fatty liver. Overfeeding of energy-rich  
270 food in ducks quickly induced non-pathogenic fatty liver. We performed full-length  
271 transcript sequencing of sibling ducks to acquire full-length transcript isoforms and to  
272 further detect ASEs. We identified 77,237 transcripts in liver from overfed ducks and  
273 69,618 transcripts in control ducks. The expressional profile and structural  
274 information of full-length transcripts were used to evaluate the relative abundance of  
275 ASEs in duck livers under different feeding conditions. The enrichment of ASEs in  
276 lipid metabolism related genes indicates transcript-level changes under the  
277 overfeeding condition.

278 Premature mRNA may produce different mature mRNA by ASEs. Our study  
279 provides us a group of differential ASEs between overfed and control ducks. ASEs  
280 with significantly differential abundance may reveal the regulation pattern of AS  
281 splicing involved in lipid metabolism. Signal peptides (16-30aa) are important in  
282 multiple fields such as protein secretion mechanisms and disease diagnosis [42].  
283 *CYP4F22* plays an important role in producing acylceramide, which is a key lipid of  
284 skin barrier in mice [43]. The loss of signal peptide of CYP4F22 protein indicates that  
285 ASEs may cause alternative protein localization to influence lipid metabolism of  
286 ducks. The *BTN* (Butyrophilin) gene family was identified in lactating mammary  
287 gland and associated with lipid secretion [38, 44]. B30.2 is a classical conserved  
288 domain of *BTN* genes, possessing multiple functions including resisting virus invasion,  
289 regulating T cell activity, and lipid secretion [45-47]. The identified transcript isoform  
290 (TCONS\_00099264) of the *BTN* family gene have lost the B30.2 domain in our study.  
291 The presence or absence of the B30.2 domain in the identified BTN protein may  
292 change the binding ability of the BTN protein. The structural changes in BTN protein  
293 products suggest that the lack of conservation of this domain or functional region is  
294 also a mode of regulation of lipid metabolism in duck liver.

295 Ducks may have unique mechanism to protect their liver from damage after lipid  
296 deposition and ASEs may play a key role in the protection process. Previous studies  
297 showed that oxidative stress induced by lipid accumulation was considered as one of  
298 the key factors for the exacerbation of NALFD [48, 49]. Glutathione (GSH) is a  
299 classical antioxidant substance, which can improve antioxidant defense ability.



300 Increasing the level of glutathione is considered as one of the methods to treat  
301 NAFLD. Mice given glycine-based treatment recover from NAFLD, with glutathione  
302 accumulating in the process of treatment, indicating that glutathione can protect liver  
303 from NAFLD [50]. The ratio of GSH/GSSG (glutathione/oxidized glutathione) is a  
304 good marker for oxidative status of cells and high level of GSSG indicates the severe  
305 steatosis and oxidative stress in liver [51]. Studies have shown that the synthetic  
306 substrates (glycine and serine) of GSH were lower, and GSH level was decreased in  
307 NAFLD patients [52]. The concentration of GSSG in human was significantly  
308 increased and the GSH/GSSG ratio was lower with NAFLD [53]. The depletion of  
309 GSH means serious oxidative stress and probable injury in human liver. However, in  
310 waterfowl such as mule ducks, GSH is not depleted during the fatty liver period and  
311 the GSH/GSSG ratio is relatively higher compared with human [54]. The different  
312 dynamics of GSH compared with human might contribute to the non-pathogenic  
313 result of fatty liver in ducks, which was different from that of human NAFLD. Among  
314 genes detected with ASEs in duck, ADH5 protect glutathione from consumption of  
315 endogenous formaldehyde [55]. We found differential ASEs in the ADH5 gene of  
316 ducks, implying that this might regulate the ADH5 protein to resist the damage of  
317 oxidation. We also found alternative splicing in GSTA2 (glutathione S-transferase  
318 alpha 2) in ducks. GSTA2 functions in oxidative stress and protects cells from  
319 oxidation through combination with GSH [56]. These results suggested that  
320 alternative splicing may enhance antioxidant ability to avoid damage form fatty liver  
321 in ducks.

322 Our studies on ASEs shed further light on regulation of lipid metabolism and  
323 GSH metabolism at the transcript level and provide us with evidence of the potential  
324 factors leading to differential fatty liver disease processes in humans.

## 325 **Conclusions**

326 Our study provides the full-length liver transcriptome of Pekin ducks to allow analysis  
327 of transcript structure. A total of 126,277 transcripts were generated and 27,317 ASEs  
328 identified, enabling us to further explore the events related to non-pathogenic fatty  
329 liver. ASEs of numerous genes involved in lipid metabolism were significantly  
330 changed by in ducks with fatty liver. Identified candidate genes *GSTA2*, *ADH5* and  
331 *DHRS2* are involved in oxidation resistance and ASEs might change their protein  
332 product to function in fatty liver process. The future challenge will be the functional  
333 validation of each transcript isoform involved in fatty liver in poultry and cross  
334 species experiments in mice. Taken together, our full-length transcriptome sequencing  
335 of overfed and control ducks enlightens us to the role of ASEs in the formation of and  
336 defense against fatty liver.

## 337 **Methods**

### 338 **Animal Feeding**

339 Five sib-pairs of 11-week-old male ducks were reared at the Jiangsu Institute of  
340 Poultry Science, China and divided into two groups. The control group were fed with  
341 180g/d (gram/day) commercial feed to 14 weeks old. The overfed group were fed  
342 with 150g corn twice a day on the first three days of the 12<sup>th</sup> week and increasing to  
343 200g twice a day on the last four days of the 12<sup>th</sup> week to adapt to the overfeeding

344 condition. After the preparation of overfeeding at the 12<sup>th</sup> week, the overfed group  
345 was fed 150g corn three time a day until 14 weeks old. After 14 weeks feeding, the  
346 sib-pair ducks were euthanized by electronarcosis and cervical dislocation and then  
347 liver tissues were collected.

#### 348 **PacBio full-length transcriptome library preparation and sequencing**

349 Library construction was performed according to the PacBio official protocol of  
350 Huada Gene Co. Ltd. BGI (Beijing, China). Total RNA was extracted from liver tissue  
351 of a sib-pair ducks from control and overfeeding groups using Trizol reagent  
352 (ThermoFisher Scientific). After quality testing, RNA was reverse transcribed into  
353 cDNA by SMARTer™ PCR cDNA Synthesis Kit (Clontech, CA, USA). Full-length  
354 transcriptomic libraries were constructed to capture complete structure information.  
355 SMART primers were incorporated and PCR was performed for single stranded  
356 cDNA and double stranded cDNA in turn. Bluepippin (Sage Science, MA, USA) was  
357 used for cDNA library length classification and PCR amplification was performed  
358 again in a different cDNA library. Sequencing adaptors were linked to cDNA, and  
359 linear DNA without adaptor was removed. Finally, after quality tests using an Agilent  
360 2100 (Agilent, CA, USA) and Qubit HS (Invitrogen, CA, USA), sequencing was  
361 carried out on the PacBio sequel platform (PacBio, CA, USA).

#### 362 **Sequence processing**

363 Full-length transcriptome raw sequencing data was strictly processed in accordance  
364 with the PacBio official smrtlink\_5.1.0 work flow ([https://www.pacb.com/support/  
365 software-downloads](https://www.pacb.com/support/software-downloads)). With this pipeline, CCS (Circular consensus sequencing) reads

366 were generated and classified into full-length non-chimeric (FLNC) and  
367 non-full-length reads. FLNC reads were then passed through ICE (Iterative Clustering  
368 for Error Correction) and input into ICE Partial and Quiver, together with  
369 non-full-length reads to acquire unpolished reads. Reads were then polished using  
370 RNA-seq data with LoRDEC software (version 0.6) with parameters -k 19, -s 3 [57].  
371 The polished reads were mapped to our recently developed high quality reference  
372 genome, SKLA1.0 (NCBI BioProject accession number PRJNA792297) by minimap2  
373 with parameter -ax splice -uf [58]. The redundant results of minimap2 were removed  
374 by cupcake (version 28.0.0) with parameter -c 0.85 -i 0.9 --dun-merge-5-shorter  
375 ([https://github.com/Magdoll/cDNA\\_Cupcake](https://github.com/Magdoll/cDNA_Cupcake)). Transcripts from ducks under different  
376 feeding conditions were merged non-redundantly for subsequent analysis. Sqanti3  
377 was used to evaluate and annotate the long-read transcriptome [59]. Sqanti3 transcript  
378 evaluation was performed using default parameters. Associated reference genes of  
379 each transcript and different types of splice junction were identified and classified by  
380 Sqanti3. Fusion transcript were also identified by Sqanti3 and the distance between  
381 transcript members in one fusion must be greater than 10,000 bp.

### 382 **LncRNA prediction**

383 CNCI (Coding-Non-Coding Index), CPC (Coding Potential Calculator) and  
384 GeneMark were used for transcript coding potential identification [60-62]. The  
385 non-coding transcripts identified by all three algorithms were filtered using thresholds  
386 of ORF<100aa and transcript length > 200nt (nucleotide). ORF sequences were  
387 acquired from transdecoder (ver 5.5.0) (<https://github.com/TransDecoder/Trans>

388 Decoder). Pfam domain and super family prediction was implemented and transcripts  
389 found by Pfam database were eliminated. A region 10,000 bp upstream and  
390 downstream of lncRNA in the DET set was regarded as the maximum cis-acting  
391 screening window, and coding genes within this range were inferred as cis-acting  
392 target genes. Pearson correlation was performed to test reliability of cis-acting pairs  
393 and the pairs within one gene range were excluded.

#### 394 **Differential transcript analysis**

395 The transcript-level expression was calculated by the Kallisto software (version 0.48.0)  
396 with default parameters based on short reads and full-length transcript sequences [63].  
397 Kallisto uses pseudoalignment framework and can quantify the expression of  
398 transcripts without additional alignment or reference genome. Transcript expression  
399 level in TPM (transcript per million) was used for significantly differentially  
400 expressed transcript screening through the sleuth R package with a threshold of  
401  $p\text{-value} < 0.01$  [64]. Differentially expressed transcripts were annotated by eggNOG  
402 webtools and GO enrichment analysis was performed by DAVID with  $FDR < 0.05$  [65,  
403 66]. KEGG enrichment analysis was performed by KOBAS online tools with  
404  $p\text{-value} < 0.01$  [67]. The data used for KEGG enrichment originates from KEGG  
405 pathway database (<https://www.kegg.jp/kegg/pathway.html>) [68].

#### 406 **Detection and analysis of alternative splicing events**

407 Alternative splicing (AS) event analysis was implemented by suppa2 software  
408 (version 2.3) with parameters: `-e SE SS MX RI -f ioe` [69]. The combination of  
409 identified ASEs and transcript-level expression were used to screen out significant

410 ASEs by suppa2 with p-value < 0.05. The Phobius software (<https://phobius.sbc.su.se/>)  
411 was used to predict transmembrane topology and signal peptides. The NCBI CDD  
412 tool was used to predict conserved domains. The protein sequences of all transcripts  
413 of fatty acid related genes with ASEs were acquired from ORFfinder and the  
414 redundant protein sequences were removed. The predicted deleteriousness of protein  
415 sequences changes was evaluated by Provean [37]. Protein sequences were  
416 downloaded from the NCBI website and multiple sequence alignment was performed  
417 using the Prank tool (version 170703).

#### 418 **List of abbreviations**

419 AS: Alternative splicing

420 lncRNA: Long noncoding RNA

421 DET: Differential expressed transcripts

422 GO: Gene ontology

423 KEGG: Kyoto Encyclopedia of Genes and Genomes

424 RNA-Seq: RNA sequencing

425 ORF: Open reading frame

426 ASEs: Alternative splicing events

427 CYP4F22: Cytochrome P450 family 4 subfamily F member 22

428 FASN: Fatty acid synthase

429 HADHB: hydroxyacyl-CoA dehydrogenase trifunctional multienzyme complex  
430 subunit beta

431 FADS: Fatty Acid Desaturase 1

432 GSTA2: Glutathione S-transferase alpha 2

433 ADH5: alcohol dehydrogenase 5 class-3

434 DHRS2: ehydrogenase/reductase 2

435 BTN: Butyrophilin

436 CPT2: Carnitine palmitoyltransferase 2

437 LIPC: Lipase C, hepatic type

438 MAPK14: Mitogen-activated protein kinase 14

439 RUBCN: Rubicon autophagy regulator

440 SOCS2: Suppressor of cytokine signaling 2

441 TSKU: Tsukushi, small leucine rich proteoglycan

442 XOR: Xanthine dehydrogenase

443 ENPP1: Ectonucleotide pyrophosphatase 1

444 SERPINA1: Serpin family A member 1

445 MGAT2: Alpha-1,6-mannosyl-glycoprotein 2-beta-N-acetylglucosaminyltransferase

446 SSU72: RNA polymerase II CTD phosphatase

447 **Declarations**

448 **Ethics approval and consent to participate**

449 All experiments were performed in accordance with the ARRIVE guidelines

450 (<https://arriveguidelines.org/>) for the reporting of animal experiments. All animals

451 used in this study were handled in strict accordance to the guidelines of the Beijing

452 Association for Science and Technology (approval ID SYXK, Beijing, 2007–0023).

453 The protocol was performed in compliance with the Beijing Laboratory Animal

454 Welfare and Ethics guidelines, as issued by the Beijing Administration Committee of  
455 Laboratory. The study was approved by the Institutional Animal Care and Use  
456 Committee of China Agricultural University (approval number:  
457 SKLAB-B-2010-003).

#### 458 **Consent for publication**

459 Not applicable.

#### 460 **Availability of data and materials**

461 The original data files have been uploaded to the NCBI SRA database. The full-length  
462 transcriptome of livers of overfed and control ducks can be accessed under accessions  
463 SRR20724681 and SRR20724682. The accession numbers for the RNA-seq data are  
464 SRR20707313-SRR20707319, SRR20707330, SRR20707341, SRR20707342.  
465 Moreover, we also generate a reviewer link  
466 (<https://dataview.ncbi.nlm.nih.gov/object/PRJNA863477?reviewer=4cr4hpi0egsuihvq>  
467 [qqeo6ctnnc](https://dataview.ncbi.nlm.nih.gov/object/PRJNA863477?reviewer=4cr4hpi0egsuihvq)). The genome draft had been assigned the following accession number  
468 JAKEIL000000000 by NCBI website (PRJNA792297,  
469 <https://dataview.ncbi.nlm.nih.gov/object/PRJNA792297?reviewer=us7cqb9blqt4v5po>  
470 [2d8rdpj77h](https://dataview.ncbi.nlm.nih.gov/object/PRJNA792297?reviewer=us7cqb9blqt4v5po)).

#### 471 **Competing interests**

472 The authors declare that they have no conflict of interest.

#### 473 **Funding**

474 This work was funded by the National Waterfowl-Industry Technology Research  
475 System (CARS-42).



476 **Authors' contributions**

477 YHH designed the project. YMW performed the transcriptomic data analyses and  
478 draft manuscript. LFS completed the smrtlink 5.1.0 pipeline. HFL, MFN, JXH, HC,  
479 WTS, DQG and LL feed animals and collected samples. MFN extracted the RNA of  
480 liver tissues. JS and YHH revised the manuscript. All authors read and approved the  
481 final manuscript.

482 **Acknowledgements**

483 We are grateful to Professor Tuoyu Geng from College of Animal Science and  
484 Technology (Yangzhou, China) and Dr. Xiaoxue Wang, Mrs Yanling Xing from State  
485 Key Laboratory for Agrobiotechnology, College of Biology Sciences, China  
486 Agricultural University for sample collection.

487 **References**

- 488 1. Riazi K, Azhari H, Charette JH, Underwood FE, King JA, Afshar EE, et al. The  
489 prevalence and incidence of NAFLD worldwide: a systematic review and  
490 meta-analysis. *Lancet Gastroenterol Hepatol.* 2022;7(9):851-861.
- 491 2. Yki-Järvinen H. Non-alcoholic fatty liver disease as a cause and a consequence  
492 of metabolic syndrome. *Lancet Diabetes Endocrinol.* 2014; 2(11):901-910.
- 493 3. Ayonrinde OT, Olynyk JK, Beilin LJ, Mori TA, Pennell CE, de Klerk N, et al.  
494 Gender-Specific Differences in Adipose Distribution and Adipocytokines  
495 Influence Adolescent Nonalcoholic Fatty Liver Disease. *Hepatology.*  
496 2011;53(3):800-809.

- 497 4. Berentzen TL, Gamborg M, Holst C, Sorensen TIA, Baker JL. Body mass index  
498 in childhood and adult risk of primary liver cancer. *J Hepatol.*  
499 2014;60(2):325-330.
- 500 5. Alsanea S, Gao M, Liu D. Phloretin Prevents High-Fat Diet-Induced Obesity and  
501 Improves Metabolic Homeostasis. *AAPS J.* 2017;19(3):797-805.
- 502 6. Hermier D, Rousselotpailley D, Peresson R, Sellier N. Influence of orotic acid  
503 and estrogen on hepatic lipid storage and secretion in the goose susceptible to  
504 liver steatosis. *Biochim Biophys Acta.* 1994; 1211(1):97-106.
- 505 7. Wei R, Han C, Deng D, Ye F, Gan X, Liu H, et al. Research progress into the  
506 physiological changes in metabolic pathways in waterfowl with hepatic steatosis.  
507 *Br Poult Sci.* 2021;62(1):118-124.
- 508 8. Davail S, Guy G, Andre JM, Hermier D, Hoo-Paris R. Metabolism in two breeds  
509 of geese with moderate or large overfeeding induced liver-steatosis. *Comp*  
510 *Biochem Physiol A Mol Integr Physiol.* 2000;126(1):91-99.
- 511 9. Hermier D, Guy G, Guillaumin S, Davail S, Andre JM, Hoo-Paris R. Differential  
512 channelling of liver lipids in relation to susceptibility to hepatic steatosis in two  
513 species of ducks. *Comp Biochem Physiol B Biochem Mol Biol.*  
514 2003;135(4):663-675.
- 515 10. Rogers TF, Palmer DH, Wright AE. Sex-Specific Selection Drives the Evolution  
516 of Alternative Splicing in Birds. *Mol Biol Evol.* 2021;38(2):519-530.
- 517 11. Zhang Y, Qian J, Gu C, Yang Y. Alternative splicing and cancer: a systematic  
518 review. *Signal Transduct Target Ther.* 2021;6(3):807-820.

- 519 12. Bhadra M, Howell P, Dutta S, Heintz C, Mair WB. Alternative splicing in aging  
520 and longevity. *Hum Genet.* 2020;139(3):357-369.
- 521 13. del Rio-Moreno M, Alors-Perez E, Gonzalez-Rubio S, Ferrin G, Reyes O,  
522 Rodriguez-Peralvarez M, et al. Dysregulation of the Splicing Machinery Is  
523 Associated to the Development of Nonalcoholic Fatty Liver Disease. *J Clin*  
524 *Endocrinol Metab.* 2019;104(8):3389-3402.
- 525 14. Wang H, Lekbaby B, Fares N, Augustin J, Attout T, Schnuriger A, et al.  
526 Alteration of splicing factors' expression during liver disease progression: impact  
527 on hepatocellular carcinoma outcome. *Hepatol Int.* 2019;13(4):454-467.
- 528 15. Baralle M, Baralle FE. Alternative splicing and liver disease. *Ann Hepatol.*  
529 2021;26: 100534-100541.
- 530 16. Li Y, Xu J, Lu Y, Bian H, Yang L, Wu H, et al. DRAK2 aggravates nonalcoholic  
531 fatty liver disease progression through SRSF6-associated RNA alternative  
532 splicing. *Cell Metab.* 2021;33(10):2004-2020.
- 533 17. Zhang Y, Chang Y, Yang T, Wen M, Zhang Z, Liu G, et al. The Hepatoprotective  
534 Effects of Zinc Glycine on Liver Injury in Meat Duck Through Alleviating  
535 Hepatic Lipid Deposition and Inflammation. *Biol Trace Elem Res.*  
536 2020;195(2):569-578.
- 537 18. Herault F, Duby C, Baeza E, Diot C. Adipogenic genes expression in relation to  
538 hepatic steatosis in the liver of two duck species. *Animal.*  
539 2018;12(12):2571-2577.
- 540 19. Jin S, Yang L, Fan X, Wu M, Xu Y, Chen X, et al. Effect of divergence in

- 541 residual feed intake on expression of lipid metabolism-related genes in the liver  
542 of meat-type ducks. *J Anim Sci.* 2019;97(9):3947-3957.
- 543 20. Jiang Y, Xie M, Fan W, Xue J, Zhou Z, Tang J, et al. Transcriptome Analysis  
544 Reveals Differential Expression of Genes Regulating Hepatic Triglyceride  
545 Metabolism in Pekin Ducks During Dietary Threonine Deficiency. *Front Genet.*  
546 2019;10:710-724.
- 547 21. Zheng J, Zhang J, Guo Y, Cui H, Lin A, Hu B, et al. Improvement on metabolic  
548 syndrome in high fat diet-induced obese mice through modulation of gut  
549 microbiota by sangguayin decoction. *J Ethnopharmacol.* 2020;246:  
550 112225-112236.
- 551 22. Liu Y-j, Li H, Tian Y, Han J, Wang X-y, Li X-y, et al. PCTR1 ameliorates  
552 lipopolysaccharide-induced acute inflammation and multiple organ damage via  
553 regulation of linoleic acid metabolism by promoting FADS1/FASDS2/ELOV2  
554 expression and reducing PLA2 expression. *Lab Invest.* 2020;100(7):904-915.
- 555 23. Hayashi Y, Shimamura A, Ishikawa T, Fujiwara Y, Ichi I. FADS2 inhibition in  
556 essential fatty acid deficiency induces hepatic lipid accumulation via impairment  
557 of very low-density lipoprotein (VLDL) secretion. *Biochem Biophys Res*  
558 *Commun.* 2018;496(2):549-555.
- 559 24. Athinarayanan S, Fan Y-Y, Wang X, Callaway E, Cai D, Chalasani N, et al. Fatty  
560 Acid Desaturase 1 Influences Hepatic Lipid Homeostasis by Modulating the  
561 PPAR alpha-FGF21 Axis. *HepatoI Commun.* 2021;5(3):461-477.
- 562 25. Gromovsky AD, Schugar RC, Brown AL, Helsley RN, Burrows AC, Ferguson D,

- 563 et al.  $\Delta$ -5 Fatty Acid Desaturase FADS1 Impacts Metabolic Disease by  
564 Balancing Proinflammatory and Proresolving Lipid Mediators. *Arterioscler*  
565 *Thromb Vasc Biol.* 2018;38(1):218-231.
- 566 26. Pan W, Ciociola E, Saraf M, Tumurbaatar B, Tuvdendorj D, Prasad S, et al.  
567 Metabolic consequences of ENPP1 overexpression in adipose tissue. *Am J*  
568 *Physiol Endocrinol Metab.* 2011;301(5):E901-E911.
- 569 27. Tsuchida T, Fukuda S, Aoyama H, Taniuchi N, Ishihara T, Ohashi N, et al.  
570 MGAT2 deficiency ameliorates high-fat diet-induced obesity and insulin  
571 resistance by inhibiting intestinal fat absorption in mice. *Lipids Health Dis.*  
572 2012;11:75-84.
- 573 28. Kim H-S, Yoon J-S, Jeon Y, Park E-J, Lee J-K, Chen S, et al. Ssu72-HNF4 alpha  
574 signaling axis classify the transition from steatohepatitis to hepatocellular  
575 carcinoma. *Cell Death Differ.* 2022;29(3):600-613.
- 576 29. Semmler G, Balcar L, Oberkofler H, Zandanell S, Strasser M, Niederseer D, et al.  
577 PNPLA3 and SERPINA1 Variants Are Associated with Severity of Fatty Liver  
578 Disease at First Referral to a Tertiary Center. *J Pers Med.* 2021;11(3).
- 579 30. Wahl MC, Will CL, Luehrmann R. The Spliceosome: Design Principles of a  
580 Dynamic RNP Machine. *Cell.* 2009;136(4):701-718.
- 581 31. Chaiyen P, Fraaije MW, Mattevi A. The enigmatic reaction of flavins with  
582 oxygen. *Trends Biochem Sci.* 2012;37(9):373-380.
- 583 32. Brubaker SW, Gauthier AE, Mills EW, Ingolia NT, Kagan JC. A Bicistronic  
584 MAVS Transcript Highlights a Class of Truncated Variants in Antiviral Immunity.

- 585 Cell. 2014;156(4):800-811.
- 586 33. Miyamoto M, Itoh N, Sawai M, Sassa T, Kihara A. Severe Skin Permeability  
587 Barrier Dysfunction in Knockout Mice Deficient in a Fatty Acid  
588 omega-Hydroxylase Crucial to Acylceramide Production. *J Invest Dermatol.*  
589 2020;140(2):319-326.
- 590 34. Datta R, Waheed A, Shah GN, Sly WS. Signal sequence mutation in autosomal  
591 dominant form of hypoparathyroidism induces apoptosis that is corrected by a  
592 chemical chaperone. *Proc Natl Acad Sci U S A.* 2007;104(50):19989-19994.
- 593 35. Bonfanti R, Colombo C, Nocerino V, Massa O, Lampasona V, Iafusco D, et al.  
594 Insulin Gene Mutations as Cause of Diabetes in Children Negative for Five Type  
595 1 Diabetes Autoantibodies. *Diabetes Care.* 2009;32(1):123-125.
- 596 36. Vezzoli V, Duminuco P, Vottero A, Kleinau G, Schuelein R, Minari R, et al. A  
597 newvariant in signal peptide of the human luteinizing hormone receptor  
598 (LHCGR) affects receptor biogenesis causing leydig cell hypoplasia. *Hum Mol*  
599 *Genet.* 2015;24(21):6003-6012.
- 600 37. Choi Y, Chan AP. PROVEAN web server: a tool to predict the functional effect  
601 of amino acid substitutions and indels. *Bioinformatics.* 2015;31(16):2745-2747.
- 602 38. Ogg SL, Weldon AK, Dobbie L, Smith AJH, Mather IH. Expression of  
603 butyrophilin (Btn1a1) in lactating mammary gland is essential for the regulated  
604 secretion of milk-lipid droplets. *Proc Natl Acad Sci U S A.*  
605 2004;101(27):10084-10089.
- 606 39. Goto M, Kitamura H, Alam MM, Ota N, Haseba T, Akimoto T, et al. Alcohol

607 dehydrogenase 3 contributes to the protection of liver from nonalcoholic  
608 steatohepatitis. *Genes Cells*. 2015;20(6):464-480.

609 40. Hayes JD, Flanagan JU, Jowsey IR. Glutathione transferases. *Annu Rev*  
610 *Pharmacol Toxicol*. 2005;45:51-88.

611 41. Yuan X, Sun Y, Cheng Q, Hu K, Ye J, Zhao Y, et al. Proteomic analysis to  
612 identify differentially expressed proteins between subjects with metabolic  
613 healthy obesity and non-alcoholic fatty liver disease. *J Proteomics*. 2020;221:  
614 103683-103692.

615 42. Owji H, Nezafat N, Negandaripour M, Hajiebrahimi A, Ghasemi Y. A  
616 comprehensive review of signal peptides: Structure, roles, and applications. *Eur J*  
617 *Cell Biol*. 2018;97(6):422-441.

618 43. Ohno Y, Nakamichi S, Ohkuni A, Kamiyama N, Naoe A, Tsujimura H, et al.  
619 Essential role of the cytochrome P450 CYP4F22 in the production of  
620 acylceramide, the key lipid for skin permeability barrier formation. *Proc Natl*  
621 *Acad Sci U S A*. 2015;112(25):7707-7712.

622 44. Franke WW, Heid HW, Grund C, Winter S, Freudenstein C, Schmid E, et al.  
623 Antibodies to the major insoluble milk fat globule membrane-associated protein:  
624 specific location in apical regions of lactating epithelial cells. *J Cell Biol*.  
625 1981;89(3):485-494.

626 45. Jeong J, Rao AU, Xu J, Ogg SL, Hathout Y, Fenselau C, et al. The  
627 PRY/SPRY/B30.2 domain of butyrophilin 1A1 (BTN1A1) binds to xanthine  
628 oxidoreductase: implications for the function of BTN1A1 in the mammary gland

629 and other tissues. *J Biol Chem.* 2009;284(33):22444-22456.

630 46. Morger D, Zosel F, Buhlmann M, Zuger S, Mittelviehhaus M, Schuler B, et al.  
631 The Three-Fold Axis of the HIV-1 Capsid Lattice Is the Species-Specific  
632 Binding Interface for TRIM5 alpha. *J Virol.* 2018;92(5): e01541-17.

633 47. Lu Y, Zhou T, Xu C, Wang R, Feng D, Li J, et al. Occludin is a target of Src  
634 kinase and promotes lipid secretion by binding to BTN1a1 and XOR. *PLoS Biol.*  
635 2022;20(1): e3001518- e3001540.

636 48. Carter-Kent C, Zein NN, Feldstein AE. Cytokines in the pathogenesis of fatty  
637 liver and disease progression to steatohepatitis: Implications for treatment. *Am J*  
638 *Gastroenterol.* 2008;103(4):1036-1042.

639 49. Reddy JK, Rao MS. Lipid metabolism and liver inflammation. II. Fatty liver  
640 disease and fatty acid oxidation. *Am J Physiol Gastrointest Liver Physiol.*  
641 2006;290(5):G852-G858.

642 50. Rom O, Liu Y, Liu Z, Zhao Y, Wu J, Ghrayeb A, et al. Glycine-based treatment  
643 ameliorates NAFLD by modulating fatty acid oxidation, glutathione synthesis,  
644 and the gut microbiome. *Sci Transl Med.* 2020;12(572): eaaz2841- eaaz2855.

645 51. Chen Y, Dong H, Thompson DC, Shertzer HG, Nebert DW, Vasiliou V.  
646 Glutathione defense mechanism in liver injury: Insights from animal models.  
647 *Food Chem Toxicol.* 2013;60:38-44.

648 52. Mardinoglu A, Bjornson E, Zhang C, Klevstig M, Soderlund S, Stahlman M, et  
649 al. Personal model-assisted identification of NAD(+) and glutathione metabolism  
650 as intervention target in NAFLD. *Mol Syst Biol.* 2017;13(3):916-932.



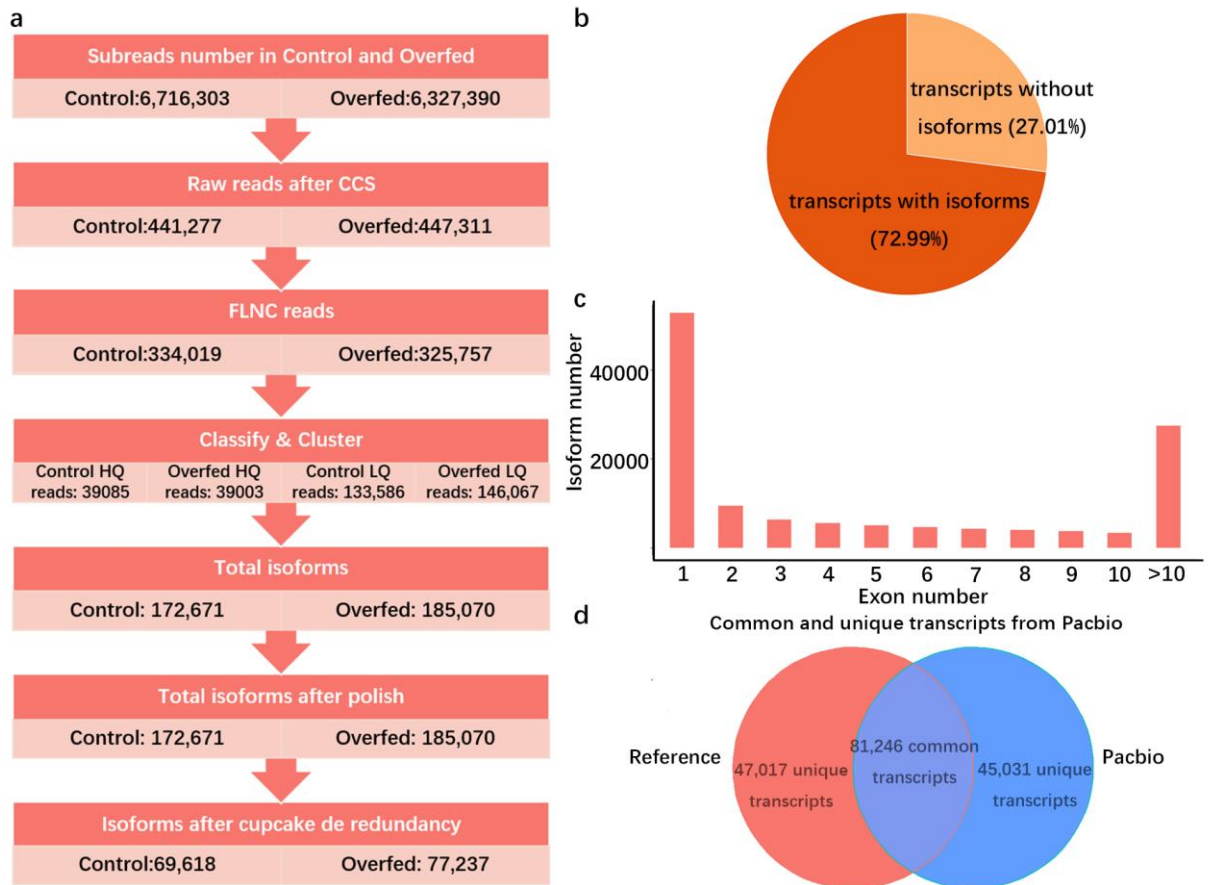
- 651 53. Hardwick RN, Fisher CD, Canet MJ, Lake AD, Cherrington NJ. Diversity in  
652 Antioxidant Response Enzymes in Progressive Stages of Human Nonalcoholic  
653 Fatty Liver Disease. *Drug Metab Dispos.* 2010;38(12):2293-2301.
- 654 54. Lo B, Marty-Gasset N, Manse H, Bannelier C, Bravo C, Domitile R, et al.  
655 Cellular markers of mule duck livers after force-feeding. *Poult Sci.*  
656 2020;99(7):3567-3573.
- 657 55. Burgos-Barragan G, Wit N, Meiser J, Dingler FA, Pietzke M, Mulderrig L, et al.  
658 Mammals divert endogenous genotoxic formaldehyde into one-carbon  
659 metabolism. *Nature.* 2017;548(7669):549-554.
- 660 56. Ng KT-P, Yeung OW-H, Lam YF, Liu J, Liu H, Pang L, et al. Glutathione  
661 S-transferase A2 promotes hepatocellular carcinoma recurrence after liver  
662 transplantation through modulating reactive oxygen species metabolism. *Cell*  
663 *Death Discov.* 2021;7(1):188-201.
- 664 57. Salmela L, Rivals E. LoRDEC: accurate and efficient long read error correction.  
665 *Bioinformatics.* 2014;30(24):3506-3514.
- 666 58. Li H. New strategies to improve minimap2 alignment accuracy. *Bioinformatics.*  
667 2021;37(23):4572-4574.
- 668 59. Tardaguila M, de la Fuente L, Marti C, Pereira C, Pardo-Palacios FJ, del Risco H,  
669 et al. SQANTI: extensive characterization of long-read transcript sequences for  
670 quality control in full-length transcriptome identification and quantification (vol  
671 28, pg 396, 2018). *Genome Res.* 2018;28(7):1096-1096.
- 672 60. Bruna T, Lomsadze A, Borodovsky M. GeneMark-EP+: eukaryotic gene

- 673 prediction with self-training in the space of genes and proteins. *NAR Genom*  
674 *Bioinform.* 2020;2(2):lqaa026-lqaa026.
- 675 61. Kong L, Zhang Y, Ye Z-Q, Liu X-Q, Zhao S-Q, Wei L, et al. CPC: assess the  
676 protein-coding potential of transcripts using sequence features and support vector  
677 machine. *Nucleic Acids Res.* 2007;35:W345-W349.
- 678 62. Sun L, Luo H, Bu D, Zhao G, Yu K, Zhang C, et al. Utilizing sequence intrinsic  
679 composition to classify protein-coding and long non-coding transcripts. *Nucleic*  
680 *Acids Res.* 2013;41(17):e166-e173.
- 681 63. Bray NL, Pimentel H, Melsted P, Pachter L. Near-optimal probabilistic RNA-seq  
682 quantification. *Nat Biotechnol.* 2016;34(5):525-527.
- 683 64. Pimentel H, Bray NL, Puente S, Melsted P, Pachter L. Differential analysis of  
684 RNA-seq incorporating quantification uncertainty. *Nat Methods.*  
685 2017;14(7):687-690.
- 686 65. Cantalapiedra CP, Hernandez-Plaza A, Letunic I, Bork P, Huerta-Cepas J.  
687 eggNOG-mapper v2: Functional Annotation, Orthology Assignments, and  
688 Domain Prediction at the Metagenomic Scale. *Mol Biol Evol.*  
689 2021;38(12):5825-5829.
- 690 66. Sherman BT, Hao M, Qiu J, Jiao X, Baseler MW, Lane HC, et al. DAVID: a web  
691 server for functional enrichment analysis and functional annotation of gene lists  
692 (2021 update). *Nucleic Acids Res.* 2022;50(W1):W216-W221.
- 693 67. Bu D, Luo H, Huo P, Wang Z, Zhang S, He Z, et al. KOBAS-i: intelligent  
694 prioritization and exploratory visualization of biological functions for gene

695 enrichment analysis. *Nucleic Acids Res.* 2021;49(W1):W317-W325.

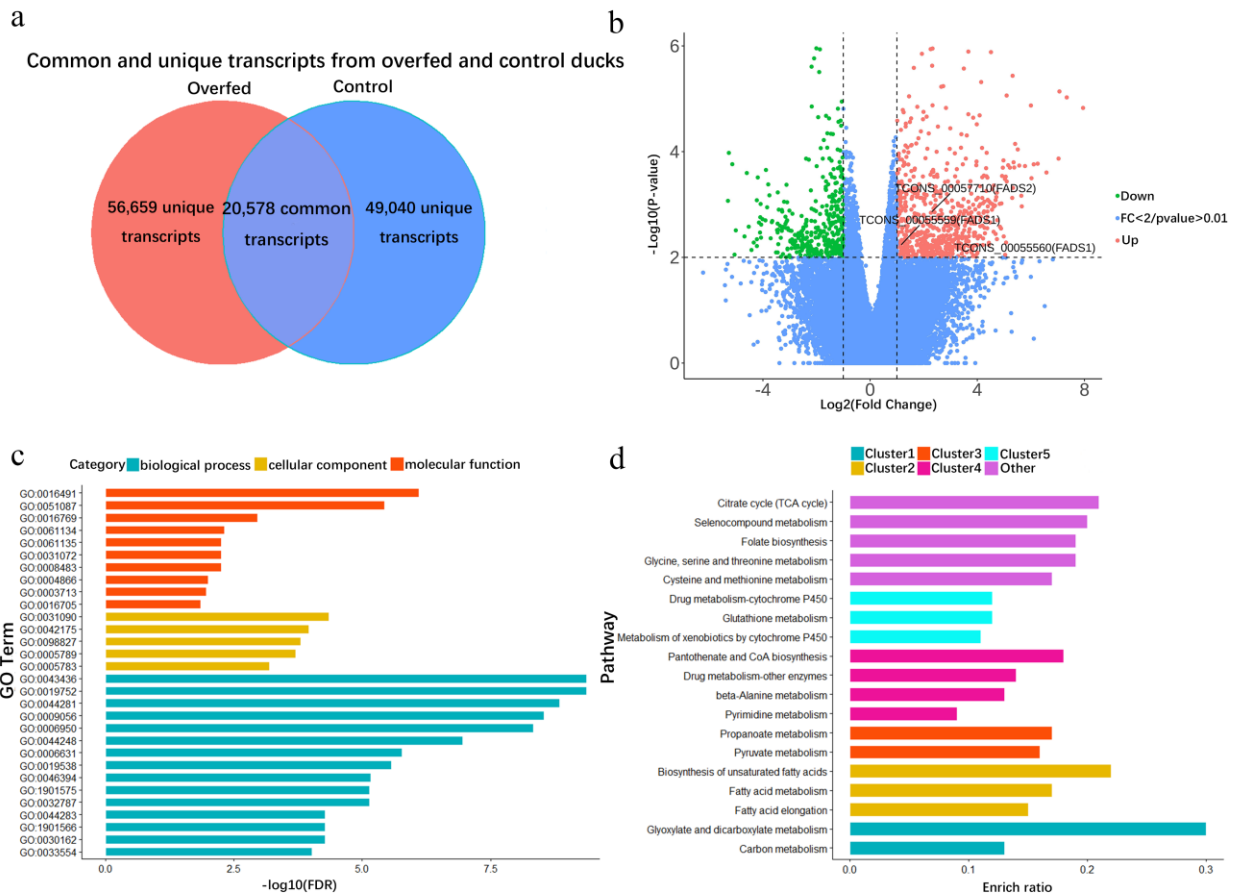
696 68. Kanehisa M, Furumichi M, Sato Y, Kawashima M, Ishiguro-Watanabe M.  
697 KEGG for taxonomy-based analysis of pathways and genomes. *Nucleic Acids*  
698 *Res.* 2023;51(D1):D587-D592.

699 69. Trincado JL, Entizne JC, Hysenaj G, Singh B, Skalic M, Elliott DJ, et al.  
700 SUPPA2: fast, accurate, and uncertainty-aware differential splicing analysis  
701 across multiple conditions. *Genome Biol.* 2018;19(1):40-50.



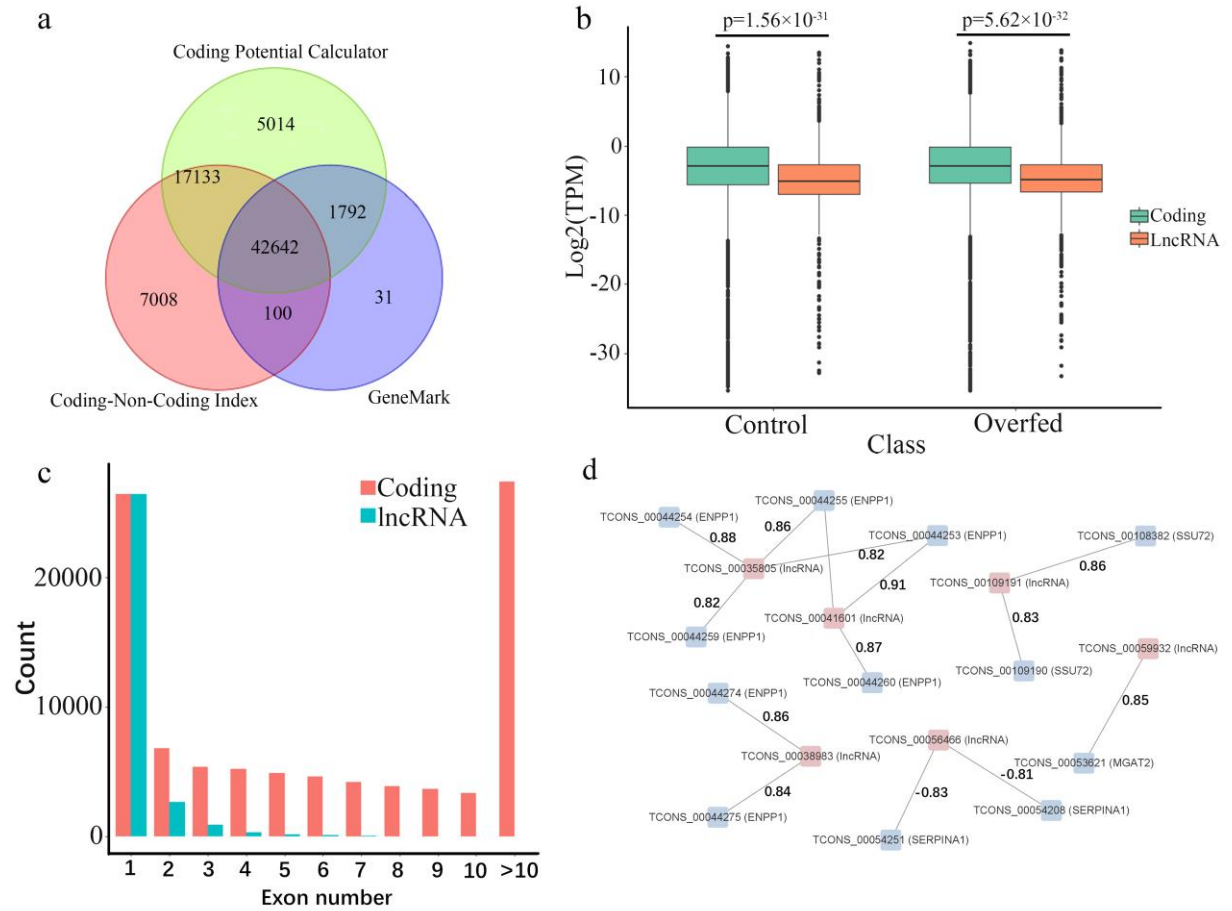
702

703 **Fig.1** Transcript processing workflow and statistics. a. Procedure of total transcripts  
 704 access for ducks. b. The ratio of transcripts with multiple isoforms and unique  
 705 transcripts without other isoforms. c. The number of transcript isoforms with different  
 706 exon number. d. Venn diagram showing common and unique transcripts with or  
 707 without reference genes.



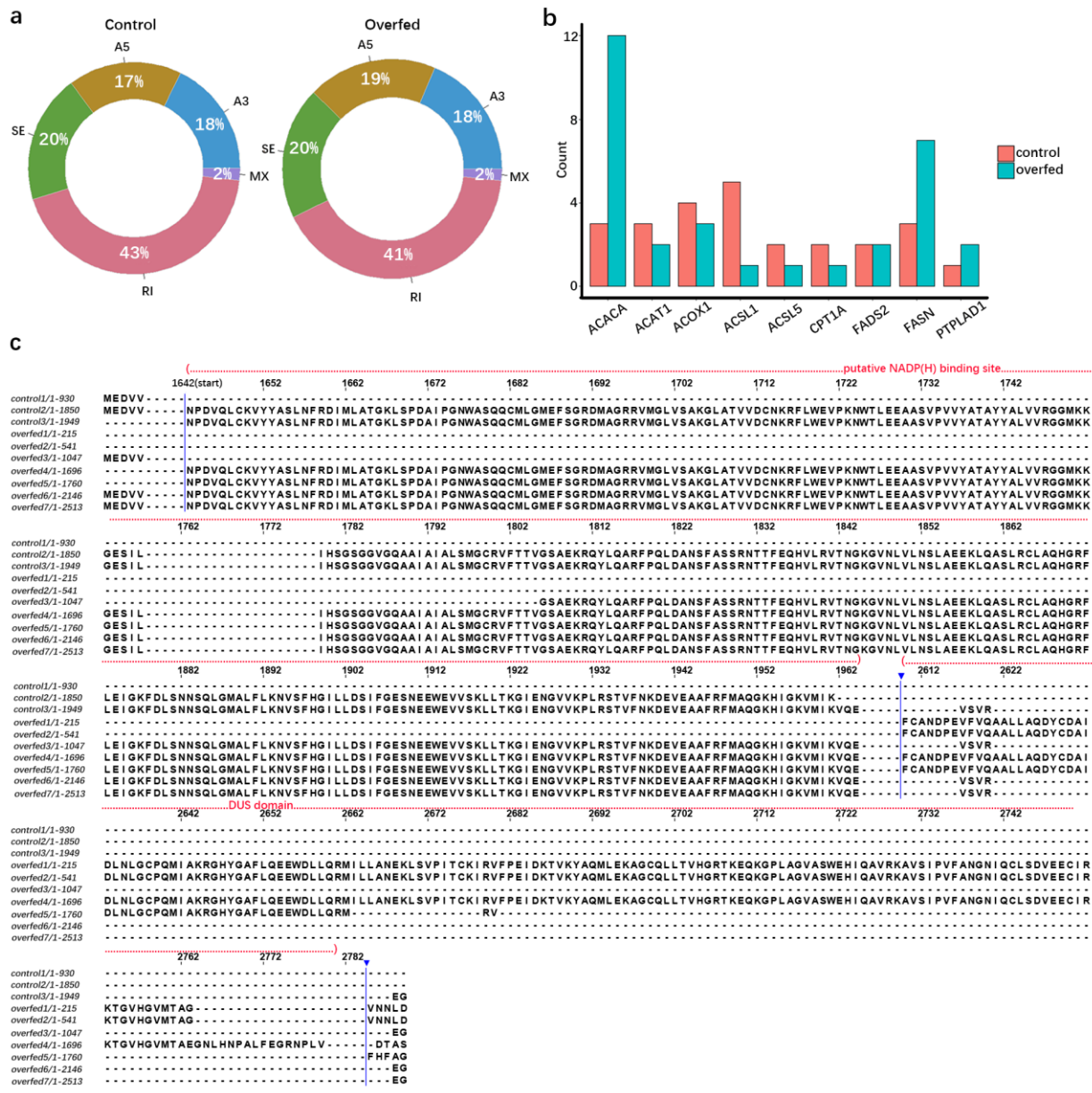
708

709 **Fig.2** Analysis of differentially expressed transcripts. a. Venn diagram of unique and  
 710 common transcripts of overfed and control groups. b. Volcano plot for differentially  
 711 expressed transcripts (FC > 2, p-value < 0.01 in up class, FC < 0.5, p-value < 0.01 in  
 712 down class). c. GO enrichment analysis of genes with significantly differentially  
 713 expressed transcripts. d. KEGG enrichment analysis of genes with significantly  
 714 differentially expressed transcripts.



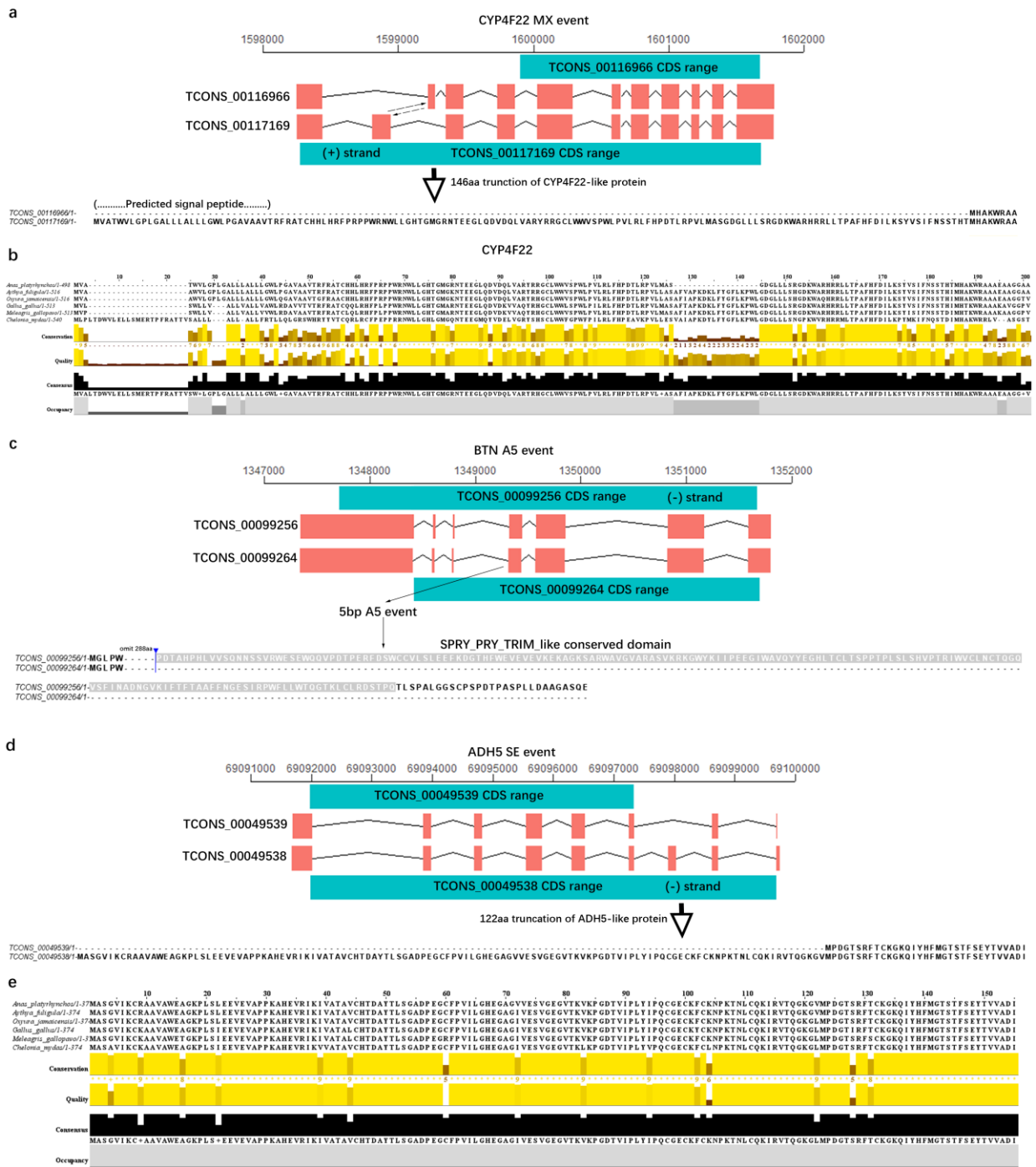
715

716 **Fig.3** Identification and characteristics of lncRNA. a. Venn diagram of non-coding  
 717 transcripts predicted by GeneMark, CPC, and CNCI. b. Expression level of transcripts  
 718 of coding genes and lncRNA in overfed and control groups. c. The number of lncRNA  
 719 with different exon number d. Correlated cis-acting pairs of DETs from lncRNA and  
 720 neighbouring coding genes within 10kb.



721

722 **Fig.4** Statistics of ASEs and analysis of ASEs in fatty acid metabolism genes. a. The  
 723 ratio of each ASEs class in overfed and control groups. b. Transcript numbers of nine  
 724 fatty acid related genes in overfed and control ducks. c. Protein sequence alignment of  
 725 FASN transcripts from overfed and control ducks.



726

727 **Fig.5** Analysis of transcripts related to lipid metabolism. a. Structural comparison of a  
 728 truncated transcript (TCONS\_00116966) and full-length CDS (TCONS\_00117169)  
 729 for the *CYP4F22* gene in ducks (the top line is chromosome coordinates axis). b.  
 730 Multiple protein sequence alignment of *CYP4F22* gene in ducks with five other birds.



731 c. Structural comparison of an A5 alternative transcript (TCONS\_00099256) and  
732 full-length CDS for *BTN* gene in ducks d. Structural comparison of a truncated  
733 transcript (TCONS\_00049539) and full-length CDS for *ADH5* gene in ducks. e.  
734 Multiple protein sequence alignment of *ADH5* gene in ducks with five other birds.

735 **Additional information**

736 Additional information accompanies this paper were list as Supplementary Figure and  
737 Supplementary Tables.